TRUCK WHEEL FATIGUE TEST SIMULATION

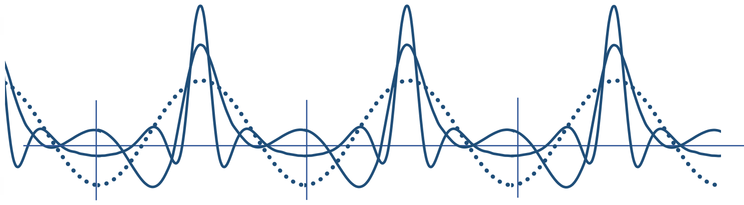

Wheel Fatigue

– Вишь ты,– сказал один другому,–
вон какое колесо! Что ты думаешь,
доедет то колесо, если б случилось
в Москву или не доедет?
– Доедет,– отвечал другой.–
А в Казань-то, я думаю, не доедет?
– В Казань не доедет,–
отвечал другой.

Н. В. Гоголь, 1835 г.

Content

FM	– Fatigue Margin
RFS	– Required Fatigue Strength
SD	– Standard Deviation of stress
σ_u	– Ultimate Tensile Strength
σ_y	– Yield Strength
E	– Young's Modulus
σ_{-1}	– Endurance Limit
A	– Fatigue Curve Parameter
B	– Fatigue Curve Parameter
T	– Material Fiber Direction (Cut Direction Transversal)
R	– Material Fiber Direction (Cut Direction Radial)
F_V	– Vertical Load Applied to the Wheel
F_H	– Horizontal Load Applied to the Wheel
M_{FS}	– Overturning Moment
μ	– Load Process Asymmetry Coefficient
σ_{max}	– Maximum Stress in a Fatigue Cycle
σ_{min}	– Minimum Stress in a Fatigue Cycle
σ_m	– Mean Stress in a Fatigue Cycle
σ_a	– Stress Amplitude of a Fatigue Cycle
σ_{eq}	– Amplitude of the Equivalent Centered Process
ψ_σ	– Coefficient Accounting for the Effect of Non-Zero Mean Stress σ_m
G	– Integral Characteristic of the Damage-Producing Portion of the Loading Process
Ps	– Probability of Failure
$K\sigma$	– Combined Correction Factor Accounting for Structural Differences
t_q	– Student's t-Distribution Quantile
C_{surf}	– Surface Finish Correction Factor
So	– Standard Deviation of the Mean Value of the Material Endurance Limit
υ_σ	– Coefficient of Variation of the Material Endurance Limit
RMS	– Root-Mean-Square Value of Positive Peaks

1. Introduction

SIMULATION OF FATIGUE TESTING OF AUTOMOTIVE WHEELS

Fatigue testing of a wheel assembly in accordance with GOST R 50511-93 (dynamic radial fatigue test with a 2° slip angle) will be performed using the following assembly:

– aluminum wheel rim 11.75 × 22.5 ST008 M22 10/335/281 ET120;

– Michelin XTE3 385/65 R22.5 tire (inflation pressure: 1.2 MPa).

The objective of this study is to evaluate the probability of successfully passing the specified fatigue test using a lightweight wheel rim design and to determine whether the proposed design modifications are acceptable.

Figure. 1. Wheel Assembly

Figure 1 shows the wheel assembly, while Figure 2 presents a cross-sectional view of the rim indicating the locations requiring mandatory fatigue strength assessment.

The analysis was performed using the **Wheel Fatigue** software package, which was originally developed for solving significantly more complex fatigue-life prediction problems involving wheel system components subjected to random dynamic loading during service in both automotive and aircraft applications.

The present task represents a particular application of this methodology and demonstrates the fatigue assessment procedure for aluminum wheel rims*.

* One of the distinguishing features of light alloys, compared with steels, is the absence of a well-defined endurance limit (σ_{-1}). As a result, fatigue damage accumulation continues even at very low stress amplitudes, which, in the case of steel wheel rims, may often be neglected during service-life assessment.

2. MINIMUM MARGINS OF SAFETY

Figure 2 shows a cross-sectional view of the wheel rim with the locations selected for fatigue assessment identified. The calculated fatigue margins for these locations are presented in Table 1.

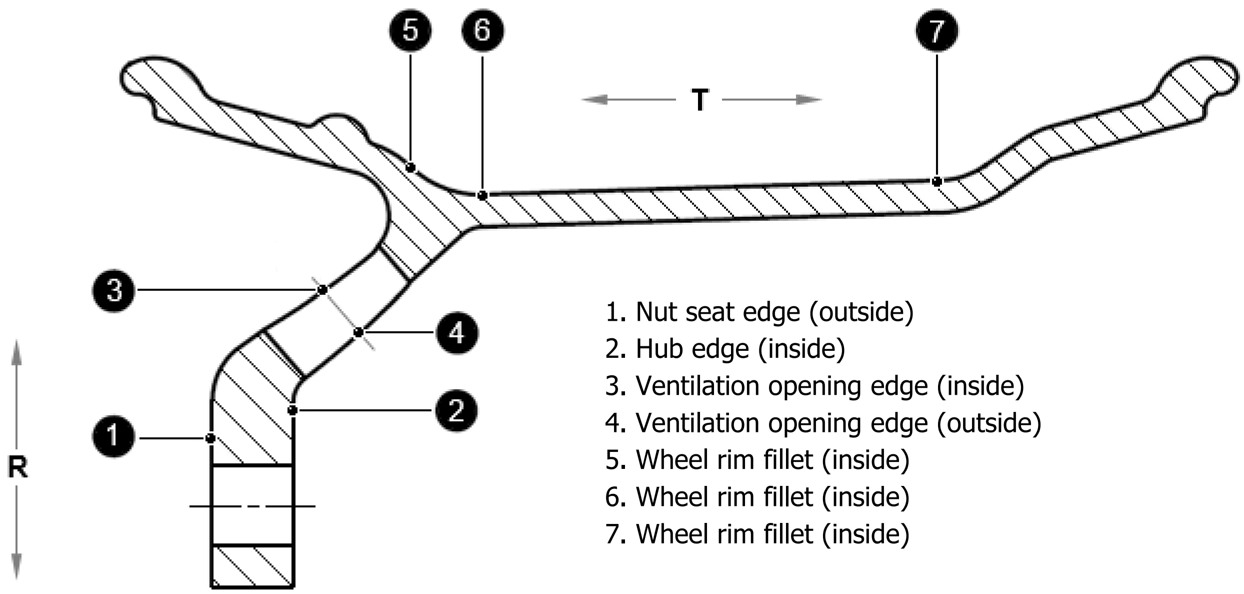

Figure. 2. Fatigue-Critical Locations in the Wheel Rim

Таблица 1. Minimum Fatigue Margins

№	SD_{eq}, MPa	Comments	$RFS_{0.1}$, MPa	Comments	FM
#1	53	see Section 5.4	81	see Section 6.2	0.54
#2	25	see Section 5.4	91	see Section 6.2	>2.00
#3	53	see Section 5.4	83	see Section 6.2	0.56
#4	79	see Section 5.4	69	see Section 6.2	-0.13
#5	19	see Section 5.4	68	see Section 6.2	>2.00
#6	21	see Section 5.4	68	see Section 6.2	>2.00
#7	34	see Section 5.4	68	see Section 6.2	0.99

$RFS_{0.1}$ corresponds to the fatigue limit state defined by a 10% probability of failure, fatigue damage D = n/N = 1.0.

Fatigue Margin defined by:

$$FM = \frac{RFS}{SD_{eq}} - 1 > 0$$

Conclusion:

The calculated fatigue margins (FM) indicate insufficient fatigue strength of the wheel rim design in several critical locations and a high probability of crack initiation during fatigue testing.

The most probable crack is expected to initiate at the inner edge of one of the ventilation openings near the end of the test.

The calculations were performed for a 90% probability of survival. If only a single wheel is planned to be tested for design validation, the probability of successfully completing the test without the appearance of a detectable fatigue crack remains low, although not negligible. Consequently, the identified design deficiencies may manifest themselves during commercial operation of the wheel rims.

To make a justified decision regarding the launch of the new wheel rim design into serial production, without revising the proposed weight-reduction measures, it is necessary to reduce the conservatism of the assumptions adopted in the analysis. In practical terms, this requires demonstrating that the calculated fatigue life represents an underestimate of the actual durability.

This will require additional monitoring of loading parameters during fatigue testing, as well as supplementary testing of laboratory specimens manufactured from the wheel rim material.

3. MECHANICAL AND FATIGUE PROPERTIES OF THE MATERIAL

The mechanical properties of the 6061-T6 aluminum alloy used for manufacturing the wheel rims are presented in Table 2.

Table 2. The mechanical properties of aluminum alloy

Direction	E, GPa	σ_y, MPa	σ_u, MPa	μ
R	68.9	270	310	0.33
T		240	270	

All properties listed in the table correspond to a temperature of 20°C.

The stress–strain curve of the 6061-T6 aluminum alloy is shown in Figure 3. The specimen extraction directions are indicated in Figure 2.

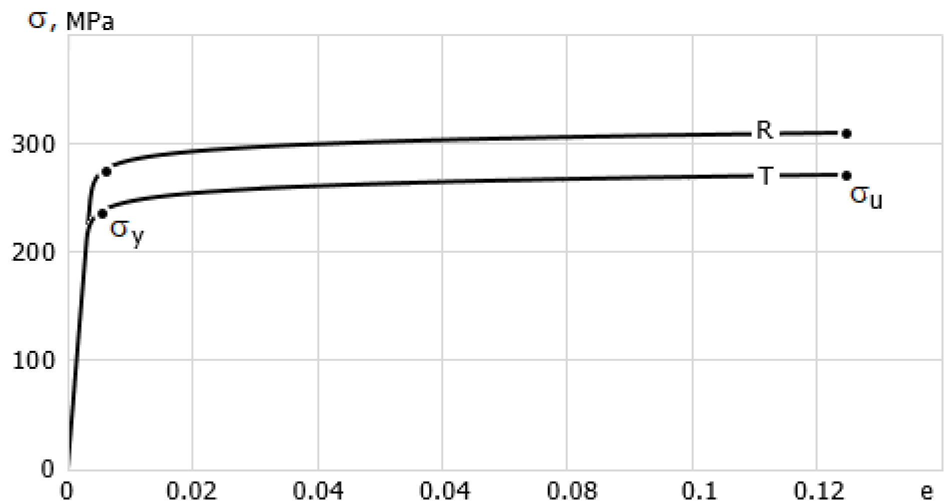

Figure. 3. Stress-Strain Curve of 6061-T6 Aluminum Alloy

The figures below present statistically derived S–N curves of laboratory specimens obtained through statistical processing of experimental fatigue test data.

The geometry of the cylindrical specimens conforms to GOST 25.502-79 (Type I). The specimens were machined from forged billets in two material orientations, R and T (see Figure 2).

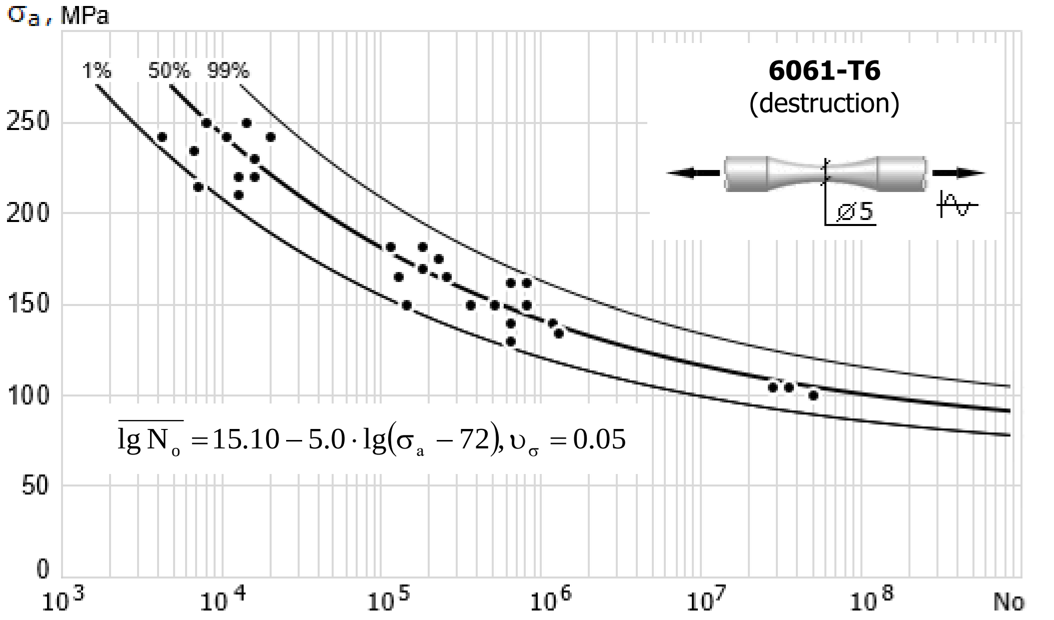

Figure. 4. S-N curve (cut direction 'T')

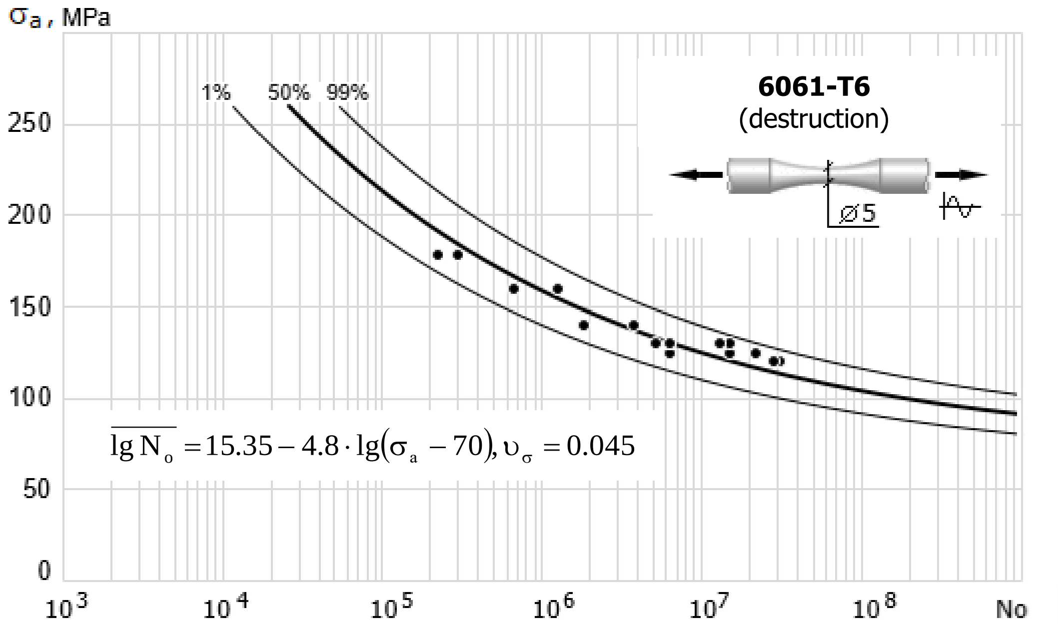

Figure. 5. S-N curve (cut direction 'R')*

All properties correspond to a temperature of 20°C.

* The number of tested specimens extracted in this direction is insufficient to provide a statistically reliable estimate of the mean endurance limit. Additional fatigue testing is therefore required. An analysis of variance (ANOVA) does not reveal a statistically significant difference between the R and T specimen populations. Consequently, the position of the corresponding S-N curve has been adjusted slightly upward in the figures to make the distinction between the two material orientations more clearly visible. Such a difference is physically expected based on the material anisotropy observed in the stress–strain curves (see Figure 3); however, it cannot be demonstrated with sufficient confidence due to the limited amount of available experimental data.

4. FATIGUE LOADS

4.1 Features of Fatigue Testing of Wheels Under Slip-Angle Conditions

The test simulates vehicle operation along a curved path in which the wheel rotation axis is not perpendicular to the direction of motion. Under such conditions, significant lateral forces may develop in the wheel rim and can become comparable in magnitude to the applied vertical load.

The standard governing wheel fatigue testing under slip-angle conditions requires the vertical load to be specified as:

$$F_V = 1.5 \cdot F_{nom} = 75kH,$$

where F_{nom} = 50kH – is the nominal wheel rim load (i.e., the maximum static load rating of the rim).

A schematic representation of the test rig, including the principal geometric dimensions and selected loading parameters, is shown in Figure 6.

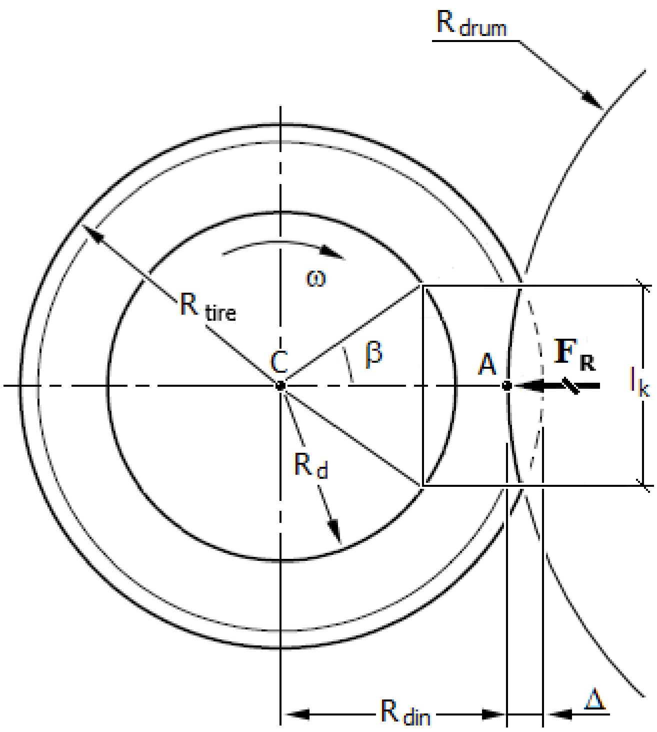

R_{drum}	= 0.8м
R_d	= 0.286м
R_{din}	=0.479м
R_{tire}	=0.529м
l_k	=460мм
β	=35^0
Δ	=50мм
F_R	=75кН
ω	=150об/мин

Figure. 6. Geometric Parameters of the Wheel and Test Rig

Regardless of the specific design of the test rig, the wheel is loaded according to the scheme shown in Figure 7. The wheel is pressed against the surface of a steel drum and accelerated to the required rotational speed, which is then maintained constant throughout the test.

The forces generated by the hydraulic actuators (F_V and F_H) are assumed to be applied at point A, which represents the geometric point of force and moment application in the test rig.

The resultant tire reactions (F_R and F_L), obtained by integrating the contact pressures over the tire contact patch area, are assumed to act at the centroid of the contact patch and are given by:

$$F_V = F_R \text{ и } F_L = F_H,$$

before:

$$F_L < \lambda \cdot F_R,$$

where λ – the rubber-to-steel friction coefficient.

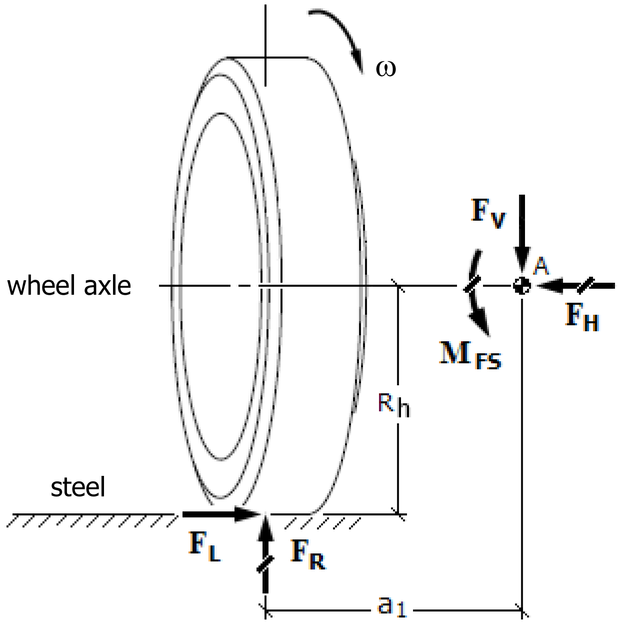

Figure. 7. Wheel Free-Body Diagram

Overturning moment is equal:

$$M_{FS} = F_L \cdot R_{din} + F_R \cdot a_1.$$

Another feature of wheel loading during the fatigue test is that the lateral force F_H is neither applied by a hydraulic actuator nor directly controlled during the test. Instead, it develops as a consequence of the prescribed slip angle α = 2° (during testing, the slip angle is defined as the angle between the drum axis of rotation and the wheel axis of rotation).

A detailed contact analysis of a tire rolling on a rigid surface under straight-line motion with a slip angle α has shown that, for a vertical load of F_V = 75kN, a drum rotational speed corresponding to a linear speed of 30km/h, and a tire inflation pressure of 1.2MPa, the resulting lateral force F_L reaches approximately 15kN* (see Section 7.1).

* This assumption should be verified during full-scale testing; a simplified 'hand' calculation based only on the tire cornering stiffness predicts a value ≈ 17кН.

4.2 Fatigue Loading Parameters

A test distance of 7,000km corresponds to 2,256,376 wheel revolutions for a wheel fitted with a 385/65 R22.5 tire, assuming an ambient air temperature of 20°C, a relative humidity of 50…60%, and a maximum wheel rim temperature below 50°C.

All loads acting on the wheel rim and required for the fatigue assessment are summarized in Table 3.

Table 3. Loads Applied to the Wheel Rim During Fatigue Testing

№	Test*	F_V, kH	F_H, kH	M_{FS}, kH·м	p, MPa	n, rotations
1	Radial Fatigue Test (α = 2^0)	75	15	7.4	1.2	2,256,376
2	Radial Fatigue Test (α = 0^0)	100	–	–	1.2	4,835,091

* Both tests were considered, but only one was described – a radial test with a 2° slip angle as more complex.

5. ANALYSIS OF THE WHEEL RIM DESIGN

5.1 Model Loading

The finite element model of the wheel rim was loaded automatically by the WHEEL FATIGUE software based on the specified loading parameters.

The generated loading conditions were verified by comparing the Totals Applied Loads reported by MSC.Patran with the reference values listed in Table 3.

An example of this verification procedure is shown in Figure 8.

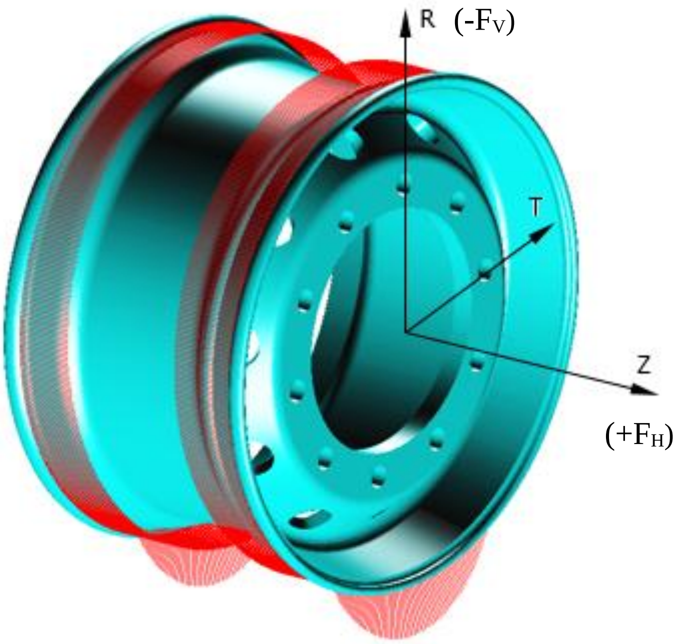

Node ID	Coord ID	Force	Moment	Fr	Ft	Fz	Mr	Mt	Mz
535789	2	616.33	0.00	0.00	0.00	-616.33	0.00	0.00	0.00
535793	2	616.63	0.00	0.00	0.00	-616.63	0.00	0.00	0.00
535797	2	616.94	0.00	0.00	0.00	-616.94	0.00	0.00	0.00
535801	2	617.24	0.00	0.00	0.00	-617.24	0.00	0.00	0.00
535805	2	617.55	0.00	0.00	0.00	-617.55	0.00	0.00	0.00
535809	2	617.87	0.00	0.00	0.00	-617.87	0.00	0.00	0.00
535813	2	618.18	0.00	0.00	0.00	-618.18	0.00	0.00	0.00
Totals	2	76473.81	7367727.00	$\boxed{74990.84}$	-0.19	$\boxed{14987.22}$	-228.01	$\boxed{7367727.00}$	0.00
				75kH		15kH		7.4kH·M	

Figure 8. Wheel Rim Model Loading and Verification of Applied Loads

5.2 Finite-Elements Analysis

The stress analysis of the wheel rim was performed at 2° increments of wheel rotation angle. A total of 180 load cases were evaluated, which is sufficient to ensure that peak stress values are not missed. The results for one of the analyzed loading conditions (load application angle equal 180°) are shown in Figure 9.

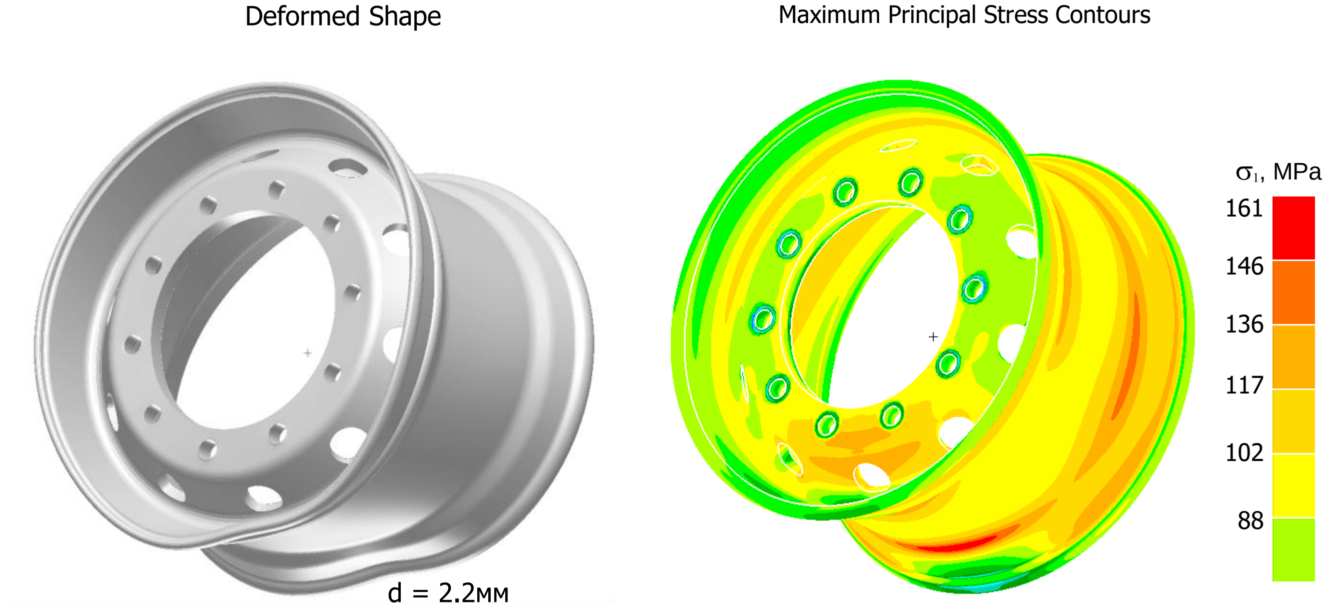

Figure 9. Wheel Rim Static Analysis Results

To verify that no fatigue-critical locations existed in the wheel rim other than those identified in Figure 2, the stress results were represented as maximum-stress-amplitude contours and compared with the Required Fatigue Strength (RFS) criterion.

At this stage, the value of RFS was fixed at 50MPa rather than calculated, based solely on the S-N curve shown in Figure 4. After all contour regions with stress amplitudes below the specified RFS level had been suppressed, the remaining areas highlighted locations where fatigue crack initiation is theoretically possible (see Figure 10). No additional fatigue-critical locations, other than those previously identified, were revealed by the analysis.

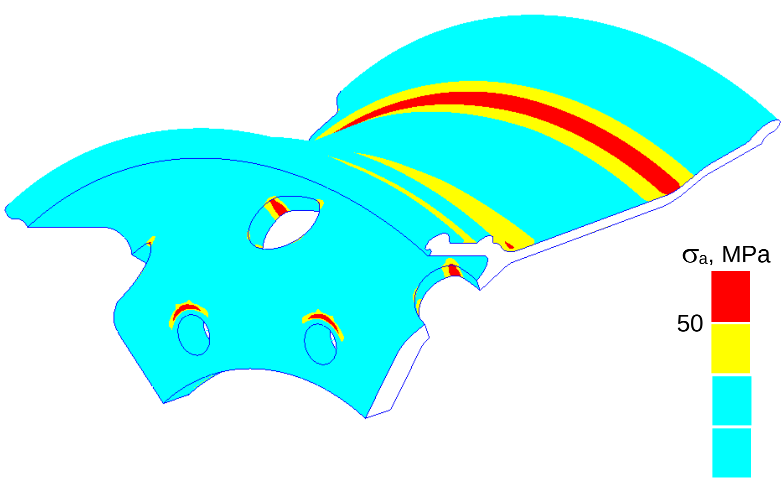

Figure 10. Contours of Maximum Principal Stress Amplitudes above RFS

5.3 Statistical Processing of the Results

Based on the generated set of numerical results, the statistical characteristics of the stress variation processes were calculated for the locations in the aluminum wheel rim identified in Figure 2.

As an example, Figure 11 shows the variation of maximum stress during wheel rotation at two points located on the outer and inner edges of a ventilation opening.

The mathematical procedure used to reduce the stress histories to two equivalent fatigue cycles is illustrated in Figure 12. Owing to the geometric symmetry of the wheel rim and the symmetry of the applied loading, the obtained solution is identical for all remaining ventilation openings; therefore, no additional analyses are required.

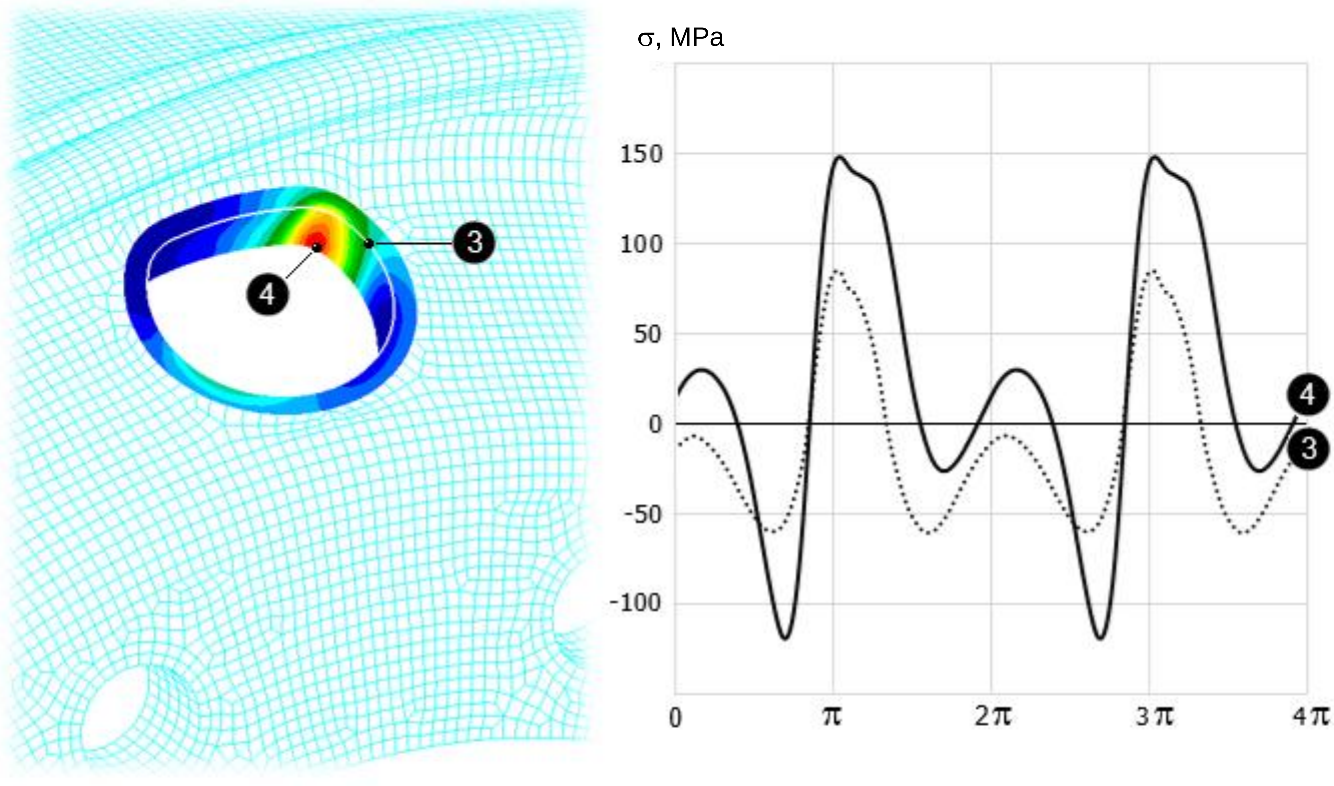

Figure 11. Stress-Time Histories (Critical Place #3 and #4) *

* The stress state at the edges of the ventilation opening is uniaxial, i.e., only one principal stress component is non-zero.

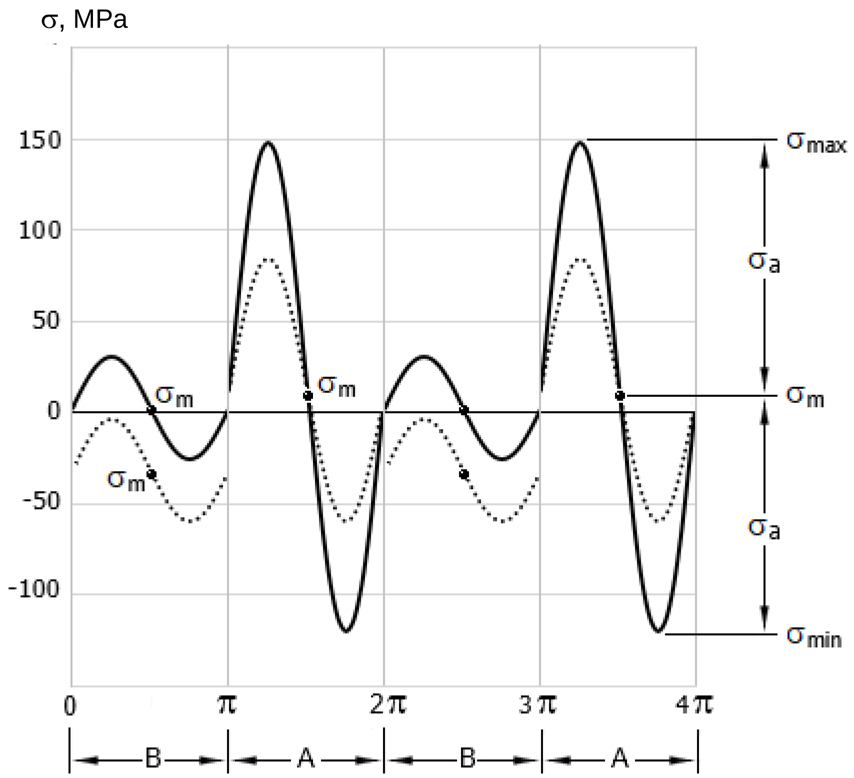

Figure. 12. Mathematical Representation of the Stress Variation Process (Locations #3 and #4)

The calculated statistical parameters of the stress variation processes at locations #3 and #4 are presented in Table 4, while the corresponding results for all fatigue-critical locations of the wheel rim (see Figure 2) are summarized in Table 5.

This approach was adopted to avoid duplication of data in two separate tables and to first introduce the procedure used to account for the effect of non-zero mean stress on fatigue damage.

Table 4. Statistical Parameters of the Stress Variation Process

№	Cycle	σ_{max}, MPa	σ_{min}, MPa	σ_m, MPa	σ_a, MPa	μ	z
#3	A	84	-60	12	72	0.24	1
	B	-7	-60	-34	27	-1.78	
#4	A	148	-120	14	134	0.15	2
	B	30	-26	2	28	0.10	
...							

$\mu = \sqrt{2} \cdot \frac{\sigma_m}{\sigma_a}$ – fatigue cycle asymmetry coefficient defined for an individual cycle (not a process);

z – number of fatigue cycles per wheel revolution.

5.4 Accounting for the Mean Stress Effect

The non-zero values of σ_m listed in Table 4 indicate the presence of a static stress offset. The asymmetry coefficient μ exceeds 0.20 in most locations; therefore, the so-called mean stress effect, resulting from the combined action of static and dynamic loads, cannot be considered negligible and must be taken into account.

This can be achieved using one of several established mean-stress correction methods, such as SWT, Gerber, Goodman, and others. The existence of multiple approaches reflects the complexity of accounting for mean stress effects and demonstrates that the accuracy of the final fatigue-life prediction may depend significantly on the selected methodology.

In the present study, the influence of loading asymmetry on fatigue life was evaluated using an approach developed by SRC (Miass, Russia), as it is specifically adapted for the analysis of aluminum-alloy structures operating under random dynamic loading conditions. The method is based on the following relationship*:

$$\sigma_{eq} = (1 + \psi_\sigma \cdot \mu) \cdot \sigma_a \tag{1}$$

where ψ_σ is a coefficient accounting for the effect of a non-zero mean stress σ_m on fatigue life. The coefficient ψ_σ is not constant. Its value reaches a maximum when the stress amplitude σ_a approaches the proportional limit of the material and decreases to a minimum as the stress level approaches the endurance limit σ_{-1}. Therefore, ψ_σ is a function of both the applied stress level and the fatigue properties of the material (see Ref. [1] for details).

If the values of ψ_σ, σ_a, and μ are known, Equation (1) can be used to determine the parameters of an equivalent centered process that produces the same fatigue damage as the actual loading process.

An example of the statistical data-processing procedure applied to the data in Table 4 is shown in Figure 13 (location #4) The resulting values of σ_{eq} are presented in Table 5. However, for the subsequent analysis, the most important result is the determination of equivalent stress standard deviation – SD_{eq}.

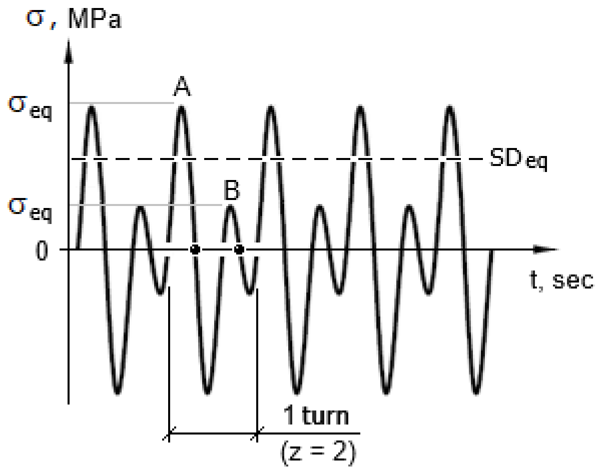

Figure 13. Equivalent Centered Stress-Time Histories

* The original equation has a different form; the expression used here is an adaptation developed for application to amplitude spectra.

Figure 14 shows the stress variation processes obtained during the simulation of fatigue testing at two locations on the wheel rim surface (Critical Location #4 and #7). These stress histories are representative of the loading conditions observed in the analyzed structure.

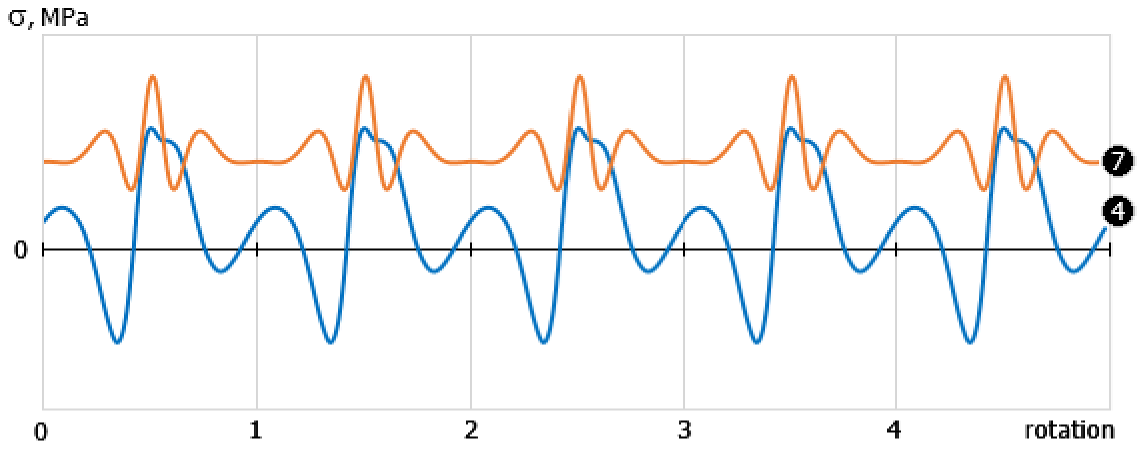

Figure 14. Stress Histories at Two Locations of the Wheel Rim

Let us begin with Process #7. It is clearly a stationary polyharmonic loading history with a significant static offset. To evaluate fatigue life, it must first be transformed into a centered loading history that is equivalent in terms of fatigue damage.

The approach used in this study constructs an equivalent loading history by centering the original signal, i.e., subtracting its mean value, followed by scaling along the stress axis. The resulting time history remains continuous and fully preserves the shape of the original process (see Curve 1 in Figure 15).

From a statistical standpoint, the original Process #7 and the equivalent centered Process 1 differ only in their stress standard deviation, and it is this parameter that will be used in the subsequent analysis.

The conventional approach to this problem is based on simplifying the loading history, for example by applying the Rainflow Counting method, followed by recalculation of the extracted cycles using one of the mean-stress correction methods.

In the example considered above, the conventional approach reduces the continuous stress history to only three fatigue cycles. These cycles are shown in Figure 15 by the dashed lines (Curve 2). The effect of mean stress has been taken into account using the Gerber correction. The difference between the two approaches is clearly visible.

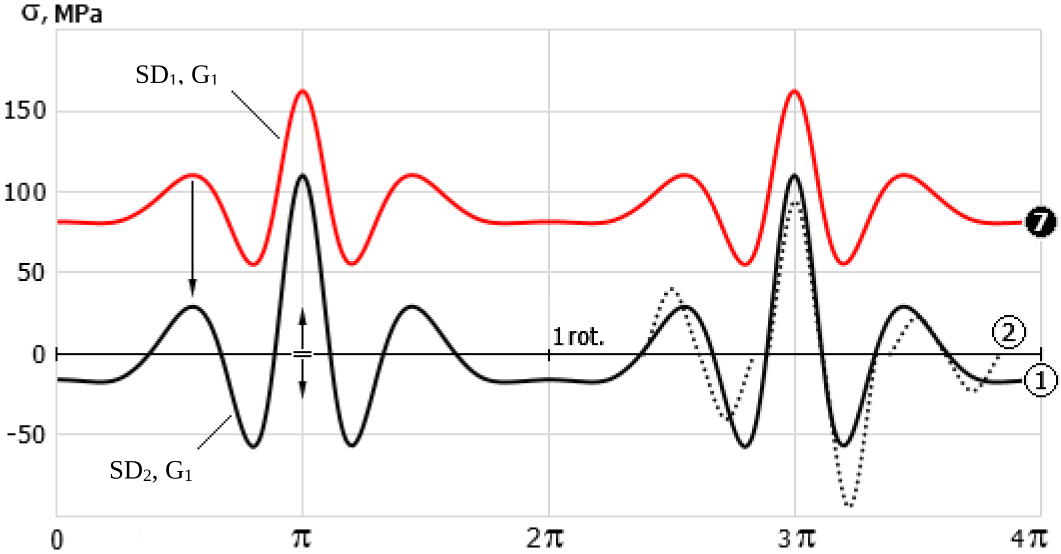

Figure 15. Creation of an Equivalent Centered Loading History

At this point, a brief digression is appropriate.

If, for any reason, one is reluctant to rely on coefficients developed more than fifty years ago in the Soviet Union - which were used in the present analysis – Figure 15 clearly demonstrates that after centering the original stress history, it can be rescaled using any widely accepted mean-stress correction method, such as Gerber, Goodman, SWT, or others.

Once this has been done, conventional fatigue analysis techniques applied to the calculated loading history will identify nearly the same fatigue cycles as those obtained from the original stress history (see Table 5, σ_{eq} vs. SWT). However, preserving the description of the loading as a continuous centered random process provides several important advantages for subsequent calculations, which will be explained in the following sections.

The calculated statistical parameters of the stress variation processes for all fatigue-critical locations of the wheel rim (see Figure 2) are presented in Table 5.

Table 5. Statistical Characteristics of the Stress Variation Processes

№	Cycle	σ_{max}, MPa	σ_{min}, MPa	σ_m, MPa	σ_a, MPa	μ	σ_{eq}, MPa	SWT, MPa	z	SD_{eq}, MPa
#1	A	128	-56	36	92	0.55	102	109	2	**53**
	B	18	11	15	3	7.07	13	7		
#2	A	9	-64	-27	37	-1.03	29	18	1	**25**
	B	-5	-64	-35	30	-1.65	20	–		
#3	A	84	-60	12	72	0.24	75	78	1	**53**
	B	-7	-60	-34	27	-1.78	17	–		
#4	A	148	-120	14	134	0.15	138	141	2	**79**
	B	30	-26	2	28	0.10	29	29		
#5	A	85	8	46	39	1.67	52	57	3	**19**
	B_2	27	10	19	9	2.99	14	16		
#6	A	113	35	74	39	2.68	60	66	3	**21**
	B_2	67	35	51	16	4.51	30	33		
#7	A	161	67	114	47	3.43	79	87	3	**34**
	B_2	114	67	91	24	5.36	50	52		

SWT – an alternative mean-stress correction method. The corresponding values are presented solely for comparison with the equivalent stress amplitudes (σ_{eq} vs. SWT) and to demonstrate the consistency of the two approaches. These values are not used in the current analysis.

The development of a fatigue loading model is typically completed by constructing a load spectrum (cycle history) describing the stress variation in the selected wheel rim locations as a non-stationary random process.

The load spectrum is constructed using the equivalent stress amplitudes obtained after accounting for the mean stress effect (σ_{eq}, see Table 5).

In the present case, it is known in advance that the stress variation process is stationary; that is, its statistical characteristics remain unchanged throughout the test, and the stress standard deviation in each location remains constant during the entire test period. Consequently, the values of SD_{eq} presented in Table 5 are already sufficient for the subsequent fatigue analysis, and the load-spectrum generation stage may be omitted.

However, even in this case, it should be emphasized that a load spectrum represents only a discretized description of the loading process and does not preserve all statistical and structural properties of the original continuous random process (i.e., it corresponds to a simplified block-loading representation).

Likewise, the stress standard deviation alone is not a sufficient parameter for a complete description of a stationary loading process; a purely harmonic process is the only exception.

Therefore, one additional step is required for a correct fatigue-life assessment. It is necessary to return to the loading processes shown in Figures 11 and 14 and consider them again, not as a sequence of two or three harmonic components, but as a single continuous process without simplifications or schematic representation.

Such an approach makes it possible to identify the systematic (structural) properties of the loading process that directly influence the rate of fatigue damage accumulation (see Section 6).

6. MATERIAL FATIGUE LIMIT STATE

The next stage of the analysis is the determination of the material's fatigue limit state.

The theory [1] used in the present work is not based on the conventional fatigue-analysis approach. It was developed specifically for evaluating the fatigue limit state of light alloys (aluminum, magnesium, etc.) subjected to random loading. Unlike traditional methods, which are based on the analysis of individual fatigue cycles, the methodology employs a statistical description of the random stress process.

In the conventional approach, fatigue life is evaluated using an S-N curve with the stress amplitude σ_a plotted on the vertical axis. In methodology [1], a fatigue curve based on the stress standard deviation (SD) is used instead.

The principal difference is that the fatigue curve is correlated not with stress amplitudes extracted sequentially from a cycle history, but with statistical characteristics of the loading process. This makes it possible to account for fatigue damage caused by stress fluctuations that would otherwise be considered non-damaging in a conventional cycle-based analysis.

The methodology is based on four numerical characteristics of a random process. However, calculations performed in the preceding stages have reduced the number of required variables to three*:

SD_{eq} – equivalent stress standard deviation characterizing the intensity of loading produced by the centered random process;

N_0 – number of zero-level crossings of the centered process with a specified derivative sign, characterizing fatigue life;

G – criterion describing the probabilistic structure of the loading process.

To describe the fatigue limit state of a material subjected to random loading, it is therefore necessary to establish a relationship involving not the two conventional parameters of stress and fatigue life, but three variables.

The input parameters for the analysis are $SDeq$ and G, while the output parameter characterizing material damageability is the number of cycles N_0 or its logarithm lgN_0.

* The mean value σ_m (static offset of the process) is incorporated into SD_{eq}.

Unlike the first two parameters, the G criterion requires additional explanation.

The calculated values of SD_{eq} (see Table 5) provide a quantitative measure of loading intensity at each investigated wheel-rim location. However, two loading processes having the same standard deviation may exhibit significantly different fatigue damage potential.

The reason is that the standard deviation characterizes only the energy level of a process and does not describe its internal structure, including the distribution of extrema, their concentration, and the statistical occurrence of the most damaging stress peaks.

Consequently, the standard deviation alone is insufficient for a complete description of the material fatigue limit state. An additional parameter is required to account for the structural properties of the loading process that govern the rate of fatigue damage accumulation.

In the methodology employed here, this role is performed by the G parameter, which represents an integral characteristic of the damage-producing portion of the loading process.

The procedure used to calculate G and subsequently incorporate it into the fatigue-curve equation as a dimensionless coefficient is explained below through a comparison of two random loading processes acting on the wheel rim: an actual service-loading process and a polyharmonic process representative of laboratory fatigue testing.

It should be noted that, within the conventional approach, the structure of the random loading process is not explicitly considered. As a result, the highest prediction accuracy can only be achieved when the S-N curve has been experimentally obtained under loading conditions identical to those experienced by the component being analyzed. In practice, however, most available S-N curves correspond to simple harmonic loading.

6.1 Structural Parameter of Random Loading

The objective of fatigue testing is to confirm the reliability and durability of the wheel rim throughout its specified service life. To achieve this, it is necessary to answer the following question: how does a successful completion of 7,000 km of fatigue testing without visible damage (i.e., without the formation of a technical crack of a specified size) correlate with the requirement for the wheel to operate for 800,000 km under real service conditions on roads of different categories?

To answer this question, the results of two analyses must be compared: 'Design Spectrum' and 'Test Spectrum'. The first characterizes the fatigue strength margins with respect to the material fatigue limit state, while the second describes the level of fatigue damage accumulated during testing.

The non-stationary random loading experienced by an automotive wheel during service is commonly simplified and represented by a so-called 'Design Spectrum'. Although such a spectrum cannot reproduce all features of real operating conditions, it provides the most accurate mathematical representation of the actual loading process. Consequently, reproducing the loading defined by the Design Spectrum would represent the most appropriate approach to laboratory fatigue testing. While technically feasible, this approach is rarely used because of the excessive test duration required.

Instead, 'Design Spectrum' is typically replaced by a simplified loading program. Among such simplified approaches, the radial fatigue test represents the most extreme simplification, replacing the actual non-stationary random loading process with a polyharmonic loading process.

This replacement must be equivalent in terms of fatigue damage. The polyharmonic loading process should either generate the same accumulated fatigue damage as 'Design Spectrum' or, at a minimum, allow the fatigue damage accumulated during testing to be evaluated with sufficient accuracy.

Figure 14 presents two stress-amplitude spectra for location #1. The first spectrum describes the stress variation over the specified service life, while the second corresponds to the stress variation accumulated during fatigue testing.

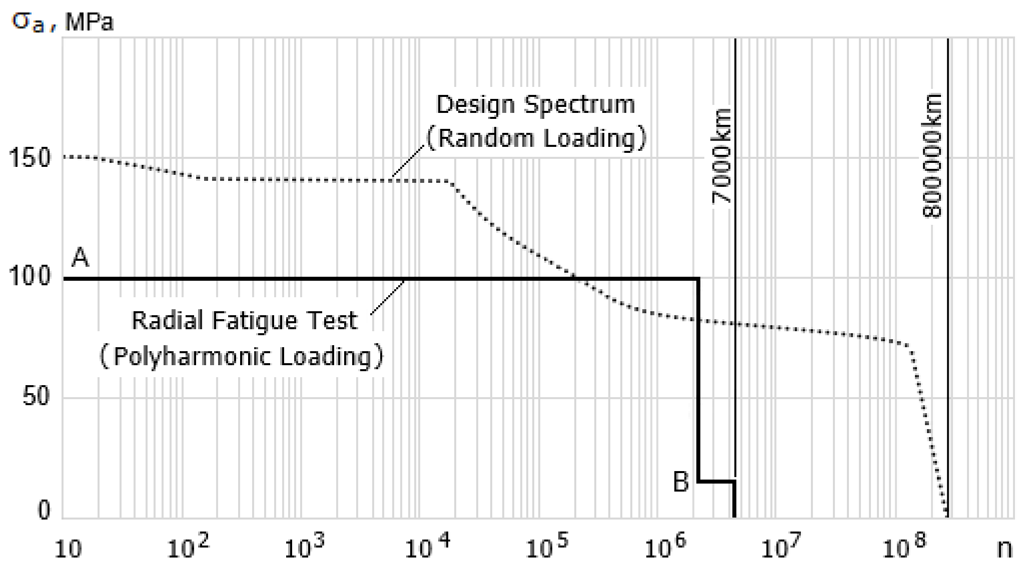

Figure 16. Stress Amplitude Spectra in the Wheel Rim (Critical Location #1)

To enable a meaningful comparison of the two loading spectra, it is first necessary to identify the structural properties of the loading processes that distinguish them from the most obvious ones – their shape and duration.

The present study is based on method for estimating fatigue durability under random vibration, proposed by N.I. Grinenko and L.A. Shefer in the early 1970s [1].

According to the research conducted by the laboratory they successively headed, specimens subjected to harmonic, polyharmonic, or random loading processes having the same loading intensity accumulate fatigue damage at different rates*. A polyharmonic loading process results in a fatigue damage accumulation rate intermediate between those of harmonic and random loading.

For wheel rims, this implies that fatigue crack initiation predicted using an S-N curve obtained under harmonic loading conditions will generally be non-conservative. Consequently, the calculated fatigue damage may be significantly underestimated.

Another important limitation is that the overwhelming majority of published S-N curves have been obtained under harmonic loading conditions, i.e., for the least damaging loading process considered in this study.

S-N curves describing the fatigue limit of a material under random stress-amplitude loading are rarely available, and obtaining them experimentally is often impractical.

As an illustrative example, Figure 15 shows two possible stress variation processes in a wheel rim: a harmonic process (Curve 1) and a polyharmonic process (Curve 2) corresponding to the amplitude spectrum presented in Figure 14.

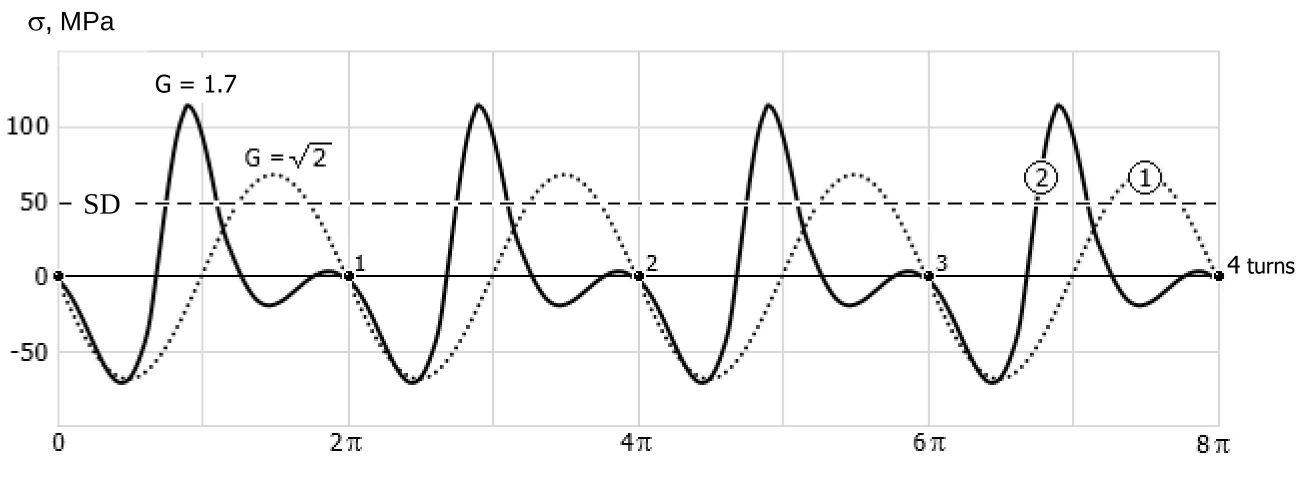

Figure 17. Comparison of Loading Processes

* The statement applies to centered loading processes having identical stress standard deviation, frequency characteristics, and structural properties.

Both processes are centered about zero and have identical standard deviations, frequency characteristics, and an irregularity factor $I = 1.00$. Nevertheless, it is evident that, despite their mathematical (statistical) equivalence, the polyharmonic process should generate greater fatigue damage during a single wheel revolution*.

It is therefore not possible to correctly evaluate the damage produced by the polyharmonic process using an S-N curve obtained under harmonic loading conditions without introducing an appropriate correction. Otherwise, the same variables would be substituted into the material limit-state equation for fundamentally different loading processes, which would lead to an incorrect fatigue-life prediction.

In the subsequent analysis, generalized material fatigue curves (see Section 3) will be used to describe the fatigue limit state. Within these curves, the differences in damage accumulation rates associated with different loading processes are accounted for through the G parameter (see Section 7.2 for details).

For loading processes with randomly varying stress amplitudes, the G parameter determines the position of the fatigue curve relative to the baseline curve, which is taken as the material S–N curve obtained under harmonic loading conditions. In other words, G provides a means of transforming the fatigue limit state corresponding to harmonic loading into the equivalent fatigue limit state associated with polyharmonic or random loading.

From a practical engineering standpoint, the G parameter establishes a relationship between the results of laboratory fatigue tests performed on material specimens and the actual operating conditions experienced by the structure.

For the fatigue test considered in this report and the polyharmonic stress variation characteristic of wheel rims, the assumption $G = 2.0$ may be regarded as sufficiently conservative. If necessary, this parameter can be verified or refined using the calculation procedure described in Section 7.2.

If only one of the two or three fatigue cycles has $\sigma_{max} > 0$ (see Curve #3 in Figure 11), the use of $G = \sqrt{2}$ is appropriate. If all fatigue cycles have $\sigma_{max} < 0$, fatigue damage accumulation at that location does not occur.

* See Forsyth's model describing the early stage of fatigue crack propagation.

The fatigue-life assessment of the wheel rim was performed for a 10% probability of failure (P_s = 0.1). As discussed in Section 5.4, this analysis is more conveniently carried out using the stress standard deviation because the stress variation processes observed during fatigue testing are stationary. Therefore, the fatigue curves obtained from laboratory specimen testing (see Figures 4 and 5) were transformed so that the vertical axis represents the standard deviation of the stress process, while the position of each curve corresponds to the specified probability of failure.

For a harmonic process, the relationship between stress amplitude and standard deviation is given by the simple expression:

$$\text{СКО} = \frac{\sigma_a}{\sqrt{2}}.$$

The resulting fatigue curves corresponding to different loading conditions are illustrated in Figure 16 using the S-N curve applied in the analysis of locations #3 through #7 as an example.

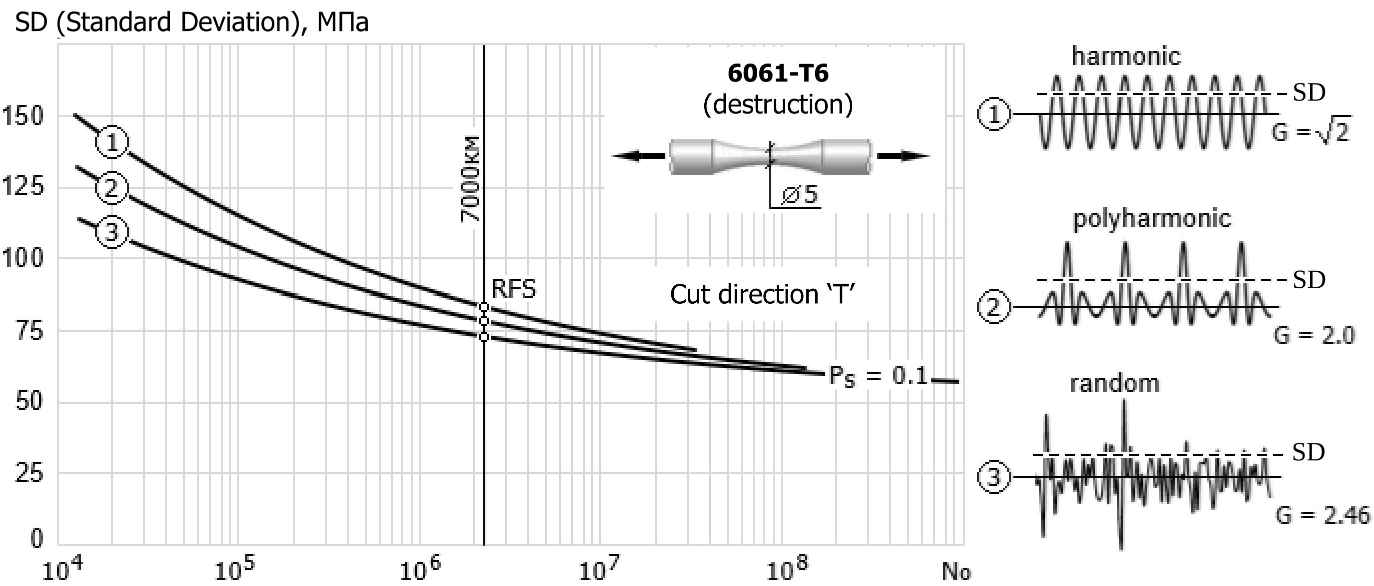

Figure. 18. Comparison of aluminum-alloy S-N curves for different loading conditions

6.2 Fatigue Strength Correction Factors

The wheel rim blank exhibits pronounced orthotropy of its fatigue properties as a direct consequence of the manufacturing process. Therefore, a separate baseline S-N curve is used for each material direction (see Figure 2), based on the fatigue characteristics of laboratory specimens presented in Section 3.

In addition to selecting the appropriate baseline fatigue curve according to the direction of the principal stresses, the following factors must be considered to correctly determine the fatigue limit state of the structure:

- geometric features of the component (i.e., differences from the laboratory specimens; see Section 7.3);
- loading characteristics (see Section 7.3);
- manufacturing-related factors (surface finish quality, local surface strengthening, etc.);
- service-related factors (environmental conditions, maximum operating temperature, radiation exposure, etc.).

The resulting correction factors, which reduce the fatigue strength of the material, are presented for all analyzed locations in Table 6.

Table 6. Parameters Defining the Fatigue Limit State of 6061-T6 Alloy

№	direction	S-N Curve[1]	K_σ [2]	υ_S [2]	C_{surf} [3]	ExPC[4]	t_q[5]	RFS[6], МПа
#1	R	$\overline{\lg N_o} = 15.35 - 4.8 \cdot \lg(\sigma_a - 70)$	1.01	0.07	0.95	1.59	1.31	**81**
#2	R		1.01	0.07	0.90	1.00	1.31	**98**
#3	–	$\overline{\lg N_o} = 15.10 - 5.0 \cdot \lg(\sigma_a - 72)$	1.10	0.10	0.95	1.00	1.31	**92**
#4	–		1.10	0.10	0.90	1.59	1.31	**69**
#5	T	$\overline{\lg N_o} = 15.10 - 5.0 \cdot \lg(\sigma_a - 72)$	1.03	0.07	0.90	1.59	1.31	**68**
#6	T		1.03	0.07	0.90	1.59	1.31	**68**
#7	T		1.03	0.07	0.90	1.59	1.31	**68**

1 – fatigue curves obtained from round laboratory specimens under harmonic tension–compression loading;
2 – calculated using the methodology of Ref. [2];
3 – no decorative surface coating is present; therefore, the values were taken from the MSC.Fatigue User's Guide ("The Effect of Surface Finish on High-Cycle Fatigue");
4 – calculated using the methodology of Ref. [1] (see Section 7.2);
5 – Student's t-distribution quantile corresponding to P = 0.1;
6 – Required Fatigue Strength (RFS) corresponding to a test mileage of 7,000km (see Figure 16).

The Required Fatigue Strength (RFS) is calculated automatically by the software using the parameters specified in Table 6.

The transformation of the laboratory-specimen fatigue curve used to obtain the material fatigue limit-state equation for Section #4 is illustrated below (the section passes through location #4 and is oriented normal to the local contour of the ventilation opening). This example provides a clear demonstration of the WHEEL FATIGUE algorithms and shows how each correction factor listed in Table 6 is incorporated into the fatigue assessment procedure.

1. $\overline{\lg N_o} = 15.10 - 5.0 \cdot \lg(\sigma_a - 72)$ – Initial S-N Curve (Ps = 0.5), T Direction

$\downarrow$

2. $\overline{\lg N_o} = 14.37 - 5.0 \cdot \lg(SD - 51.4)$ – After Conversion from Amplitude to SD (Ps = 0.5)

$\downarrow$

3. $\overline{\lg N_o} = 14.57 - 5.0 \cdot \lg(SD - 56.6)$ – After Accounting for Structural Differences ($K\sigma$ = 1.1)

$\downarrow$

4. $\overline{\lg N_o} = 14.34 - 5.0 \cdot \lg(SD - 51)$ – After Accounting for Surface Finish Effects (C_{surf} = 0.9):

$\downarrow$

5. $\overline{\lg N_o} = 13.35 - 5.0 \cdot \lg(SD - 51)$ – After Accounting for Random Loading Effects (ExPC = 1.6)

$\downarrow$

6. $\lg N = 13.27 - 5.0 \cdot \lg(SD - 48.4)$ – Final S-N Curve (Ps = 0.1, tq = 1.31, υ_s = 0.10)

According to the final S-N curve, the standard deviation of the stress process at Location #4 shall not exceed 69MPa in order to achieve a test mileage of 7,000km (2,256,376 wheel revolutions; see Table 3) at the specified probability level.

The calculated fatigue margins and the resulting assessment are summarized in Section 2.

List of Sources

1. Grinenko, N.I., and Shefer, L.A. A Spectral Method for Fatigue Life Assessment under Random Loading. Problemy Prochnosti (Strength of Materials), No.1, 1976, pp. 19–22.

2. Menshikov, S.Y. Probabilistic Method for Evaluating Fatigue Resistance Characteristics of Structural Components. PhD Thesis Abstract, Chelyabinsk, 1989, 16p.

7. APPENDIX

7.1 Results of the Nonlinear Finite Element Analysis

The lateral force F_L corresponding to different slip angles α, for a specified vertical load F_V and known tire characteristics (see Figure 19), was determined by solving the contact problem of a wheel rolling with a slip angle on a rigid surface.

A nonlinear finite element analysis of the tire was performed. The model accounted for the nonlinear mechanical behavior of rubber, internal steel reinforcement, tire inflation pressure, wheel rotational speed, tread pattern geometry, and other relevant factors. A detailed description of the finite element model, the kinematic assumptions employed, and the simplifications adopted is beyond the scope of the present report. For the purposes of this study, the key conclusions and their validity are of primary importance.

The initial analysis was performed using a friction coefficient of λ = 0.85 (rubber/asphalt contact). After adjustment of several constants in the Mooney–Rivlin constitutive model and recalculation of the stiffness characteristics of certain finite elements, satisfactory agreement between the numerical predictions and the available experimental data was achieved.

A second analysis was then performed using a reduced friction coefficient of λ = 0.22. Under these conditions, the calculated lateral force F_L at a slip angle of 2° was approximately 15kN.

The calculation results are presented in the form of two graphs in Figure 17.

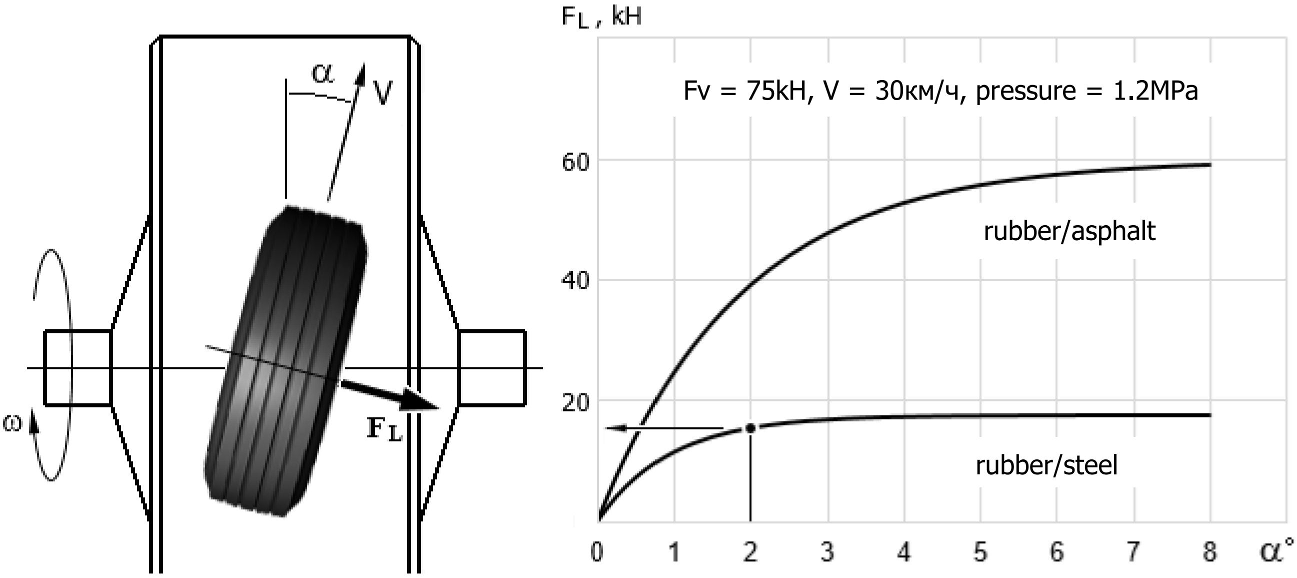

Figure 19. Results of the Nonlinear Analysis of the Wheel Assembly Model

7.2 Calculation of ExPC* Parameter for Polyharmonic Process

The fatigue curves of identical specimens subjected to harmonic and random loading do not coincide. The parameter G provides a means of quantifying this discrepancy, namely, the extent to which the fatigue curve corresponding to random loading is shifted downward relative to the baseline S-N curve obtained under harmonic loading.

For a polyharmonic stress history, the parameter G can be determined without solving a system of integral equations. If the continuous loading history is represented by only three harmonic components (see Figure 20), each containing the same number of cycles (i.e., z = 3), the governing equations can often be simplified to the following expression:

$$G = \frac{\sigma_{max}}{СКО} \cdot \frac{RMS_{max}}{RMS_{(+)}} \cdot \frac{n_{max}}{n_{(+)}} = \frac{1}{3} \cdot \frac{\sigma_{max}}{СКО} \cdot \frac{RMS_{max}}{RMS_{(+)}} \quad (2)$$

As an example, Figure 20 presents the statistical analysis of the loading history represented by Process 7 in Figure 14. The results of the calculations are summarized in Table 7, where all variables appearing in Equation (2) are also defined.

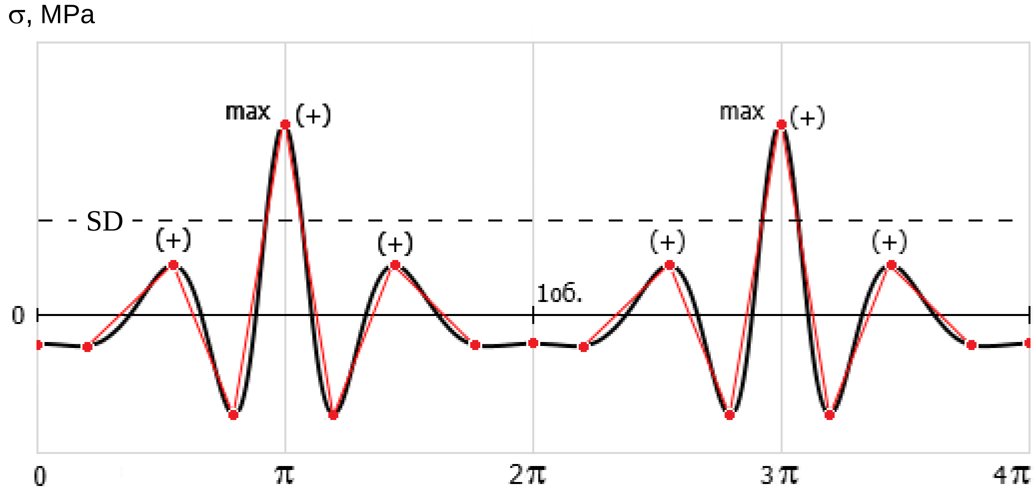

Figure 20. Polyharmonic Stress History

* The name of this parameter was suggested by an AI, which argued that the original designation didn't adequately reflect its physical meaning, whereas the abbreviation ExPC (Extreme Peak Concentration Factor) describes the parameter more clearly and accurately. Rather than resisting useful terminology, we adopt the ExPC notation throughout this paper. However, it should be emphasized that the interpretation of the parameter, its mathematical formulation, and its original designation were first proposed in Reference [1].

Table 7. Structural Parameter G calculation

Symbol	Value	Unit	Comments
σ_{max}	111	MPa	Maximum Stress
СКО	32	MPa	Process Standard Deviation
σ_m	0	MPa	Mean Stress
$n_{(+)}$	3	cycle	Relative Number of Positive Peaks
n_{max}	1	cycle	Relative Number of Damaging Peaks
$RMS_{(+)}$	68.5	MPa	RMS of Positive Peaks
RMS_{max}	111	MPa	RMS of Damaging Peaks
G	1.88		Structural Parameter

Applying the same procedure to Process 4 (see Figure 14) yields a structural parameter value of G = 1.71.

The practical application of the parameter G is demonstrated below using two centered stress histories shown in Figure 21. Their shapes are fully analogous to those discussed above.

Curves 1 and 2 in Figure 21 represent stationary random stress histories measured at two locations on the surface of the wheel rim during bench fatigue testing.

Curve 3 represents the harmonic stress history experienced by laboratory specimens during fatigue testing.

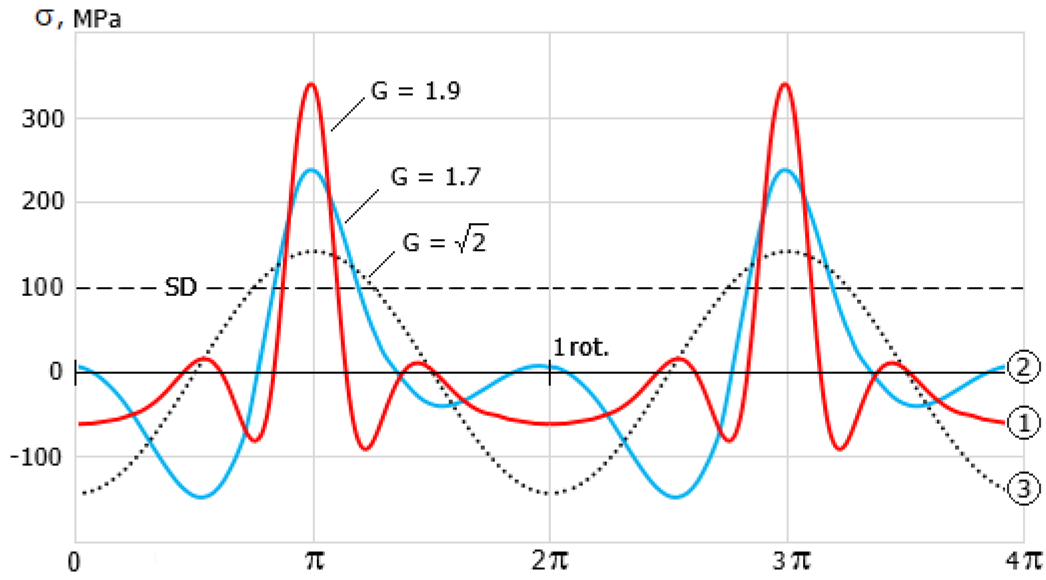

Figure 21. Stress Variation in the Wheel Rim

All curves are schematic. For clarity and ease of comparison, they are presented so that the absolute maxima of all three processes occur at the same phase angle. In addition, they have been scaled so that the stress standard deviation of each process over one-wheel revolution is equal to 100MPa. This scaling does not affect the value of the parameter G.

The three stress histories differ in shape, maximum stress, and the number of fatigue loading cycles. Nevertheless, from a statistical point of view, they are nearly equivalent: all are stationary, centered about zero, have a stress standard deviation of 100MPa, and an irregularity factor of 1.00. The only parameter distinguishing these processes is G.

The physical meaning of G is to quantify the concentration of damaging stress peaks within the loading history. Even when different loading processes have the same energy level (i.e., the same stress standard deviation), they may differ significantly in the frequency of occurrence and magnitude of extreme stress peaks responsible for fatigue damage accumulation.

Therefore, the larger the value of G, the greater the concentration and/or intensity of damaging stress peaks and, consequently, the fewer wheel revolutions (fatigue loading cycles) the structure can withstand before failure.

For use in fatigue analysis, the structural parameter G is converted to the dimensionless coefficient ExPC, which quantifies the relative increase in fatigue damage relative to a reference loading process. The reference is taken to be harmonic loading, for which the value of G is constant and equal to $\sqrt{2}$. The increase in the damaging effect of a random loading process relative to the harmonic one is determined as follows:

$$\mathrm{ExPC}_i = \frac{G_0 - \sqrt{2}}{G_0 - G_i};$$

where Go is a material constant. For most aluminum alloys, its value lies within the range of 3.7...4.3. In practical applications, Go = 4.0 is generally adopted. However, the selection of its exact value depends on the material and on accumulated experience with the proposed methodology.

To account for the effect of random loading, the position of the material S-N curve is adjusted according to the calculated ExPC value using the following equation:

$$\overline{\lg N_i} = A - B \cdot \lg\left[ExPC_i \cdot \left(CKO_i - S_0\right)\right];$$

where:

A and B – the parameters of the S–N curve (under harmonic loading);

S_0 – the mean value of the standard deviation corresponding to the fatigue endurance limit.

The resulting fatigue curves are shown in Figure 22.

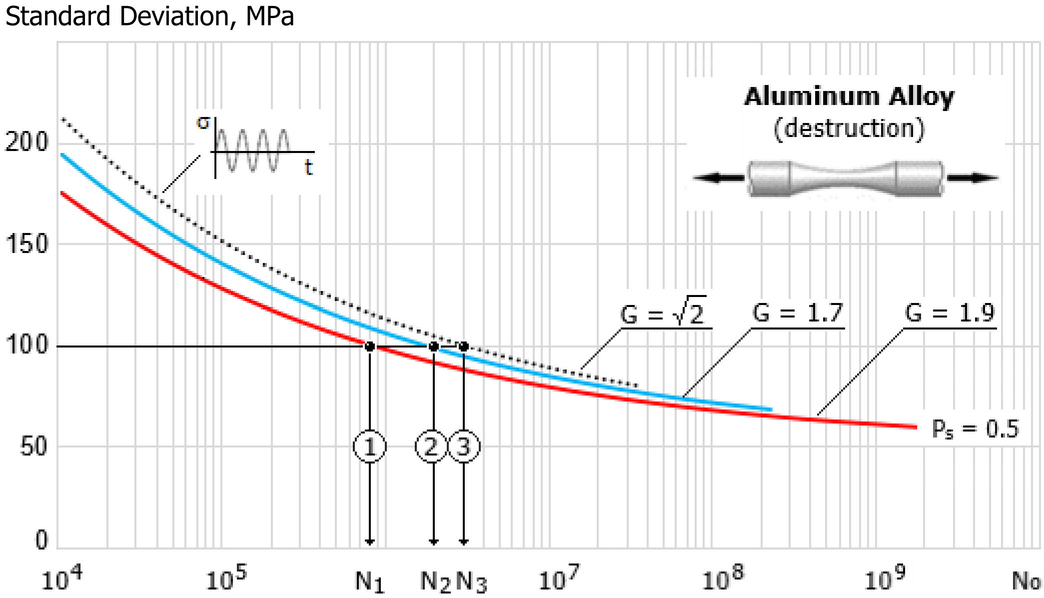

Figure 22. S-N Curves of the Aluminum Alloy under Different Loading Conditions

$SD_1 = SD_2 = SD_3$; $G_1 > G_2 > G_3$; $N_1 < N_2 < N_3$

7.3 Accounting for Structural Differences

Accounting for Structural Differences Between the Wheel Rim Components and the Tested Laboratory Specimens Was Performed Using the Method Proposed by S.Y. Menshikov [2].

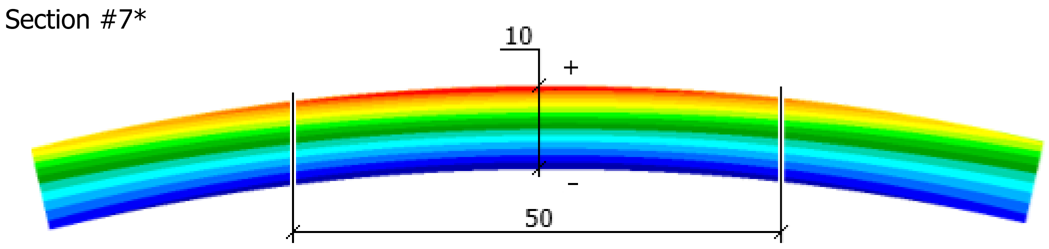

Bending Stress Contours

* The section passes through Location #7 and is oriented perpendicular to the wheel axis of rotation

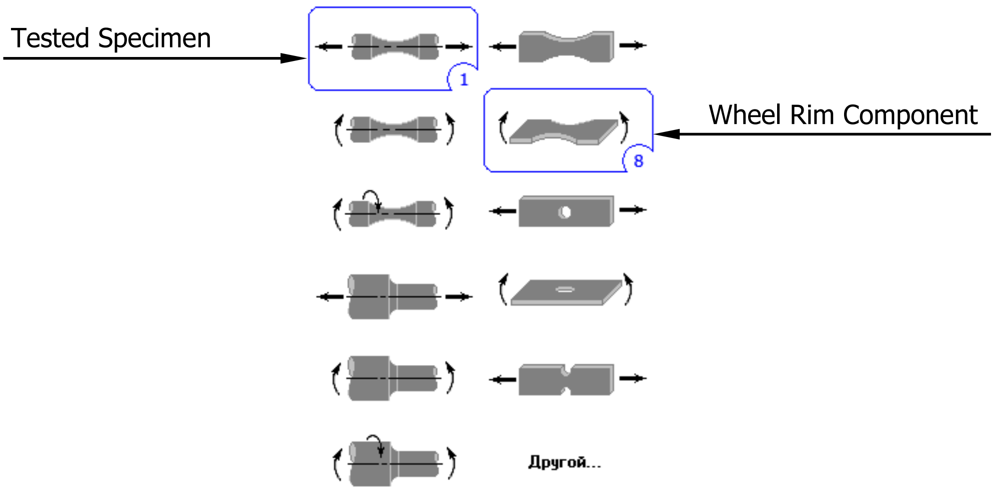

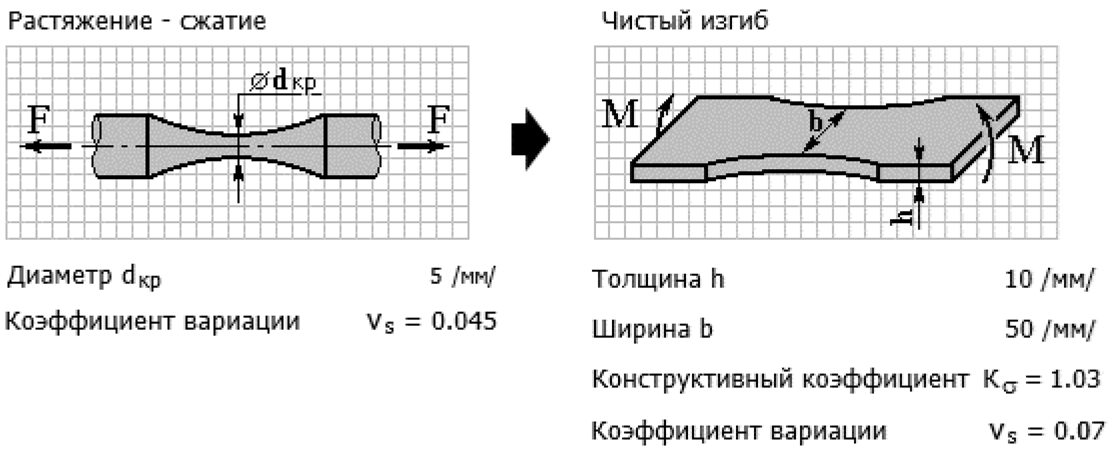

Figure 23. Accounting for Structural Differences (Critical Locations #5, #6, and #7)

7.4 Surface Finish Effects

Figure 24 presents the surface-finish correction factor (C_{surf}) as a function of the surface quality of 6061-T6 aluminum alloy. The correlation is applicable within the fatigue-life range of 10^5–10^7 cycles.

Figure 24. C_{surf} of 6061-T6 aluminum alloy

The fatigue-life assessment of wheel rims under random dynamic operating loads requires the evaluation of numerous interacting factors and is typically based on several dozen individual analyses. The example presented above illustrates only one element of the overall methodology. Further details are available at the link below.

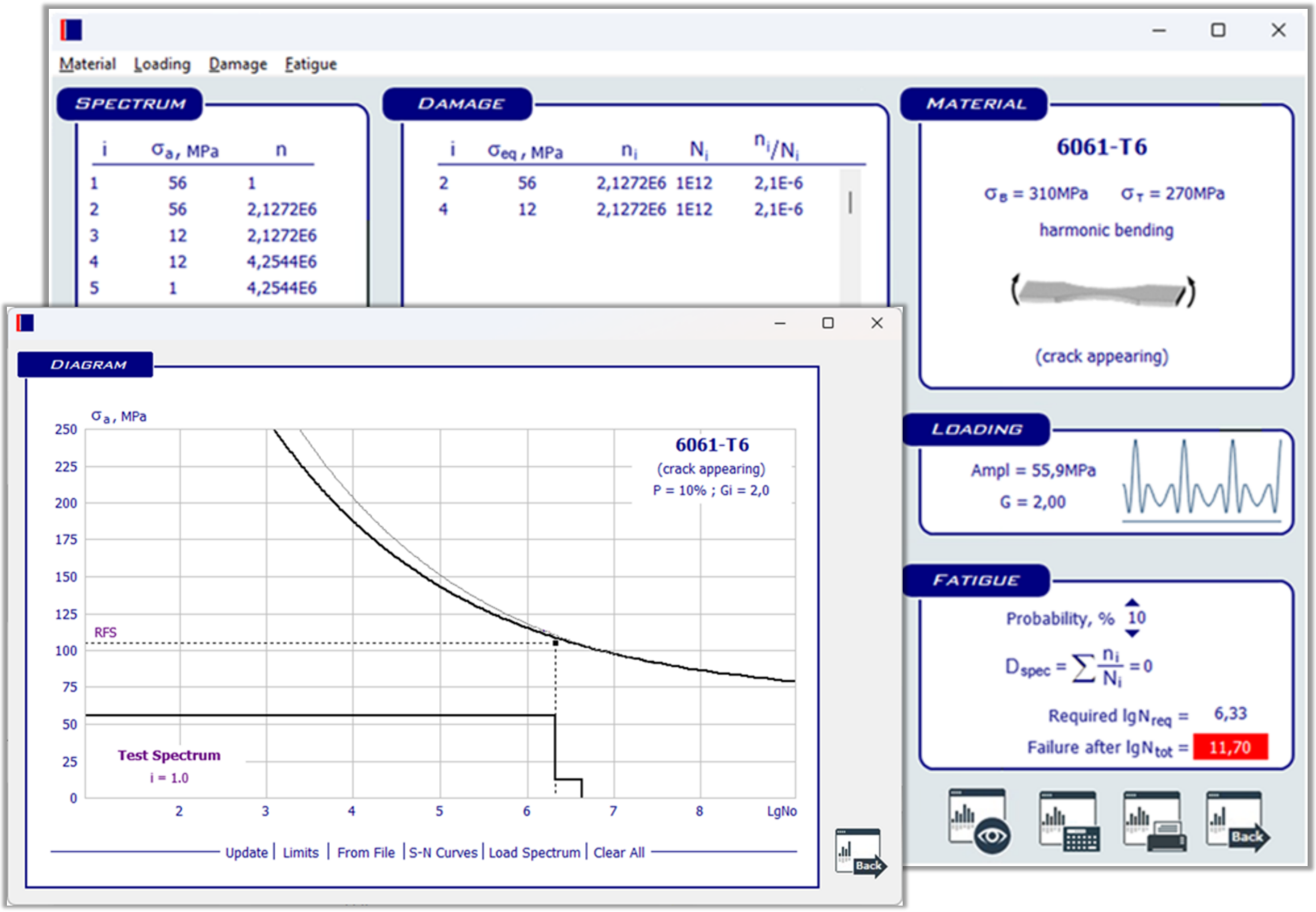

Figure 25. An example of the Wheel Fatigue operation

We openly describe the methodologies used and are prepared to discuss any aspect of the fatigue analysis procedure in detail. However, the purpose of this article is to demonstrate the true complexity of such assessments. Fatigue analysis is not merely a collection of equations but a comprehensive engineering task that requires the consistent execution of numerous interrelated steps. As a result, practical experience often has as much influence on the accuracy of the final result as the analytical models themselves.

By engaging our specialists, you obtain not only a completed analysis but also confidence that the assumptions adopted are appropriate, the methodology has been applied correctly, and the resulting conclusions are technically justified.